

BRIEF COMMUNICATION

Short pulse width widens the therapeutic window of subthalamic neurostimulation

Martin M. Reich^{1,a}, Frank Steigerwald^{1,a}, Anna D. Sawalhe¹, Rene Reese¹, Kabilar Gunalan², Silvia Johannes³, Robert Nickl³, Cordula Matthies³, Cameron C. McIntyre² & Jens Volkmann¹

¹Department of Neurology, Julius-Maximilians-University, Würzburg, Germany

²Department of Biomedical Engineering, Case Western Reserve University, Cleveland, Ohio

³Department of Neurosurgery, Julius-Maximilians-University, Würzburg, Germany

Correspondence

Jens Volkmann, Department of Neurology, Universitätsklinikum Würzburg, Josef-Schneider-Str. 11, D-97080 Würzburg, Germany. Tel: +49 (931)20123751; Fax: +49 (931)20123946; E-mail: volkmann_j@klinik.uni-wuerzburg.de

Funding Information

The study was funded by an IZKF grant (N-215) to JV from the University of Würzburg.

Received: 24 July 2014; Revised: 9 December 2014; Accepted: 10 December 2014

Annals of Clinical and Translational Neurology 2015; 2(4): 427–432

doi: 10.1002/acn3.168

^aThese authors contributed equally.

Abstract

We explored the impact of pulse durations $<60 \mu\text{sec}$ on the therapeutic window of subthalamic neurostimulation in Parkinson's disease. Current thresholds for full rigidity control and first muscle contractions were evaluated at pulse durations between 20 and 120 μsec during a monopolar review session in four patients. The average therapeutic window was 2.16 mA at 60 μsec , which proportionally increased by 182% at 30 μsec , while decreasing by 46% at 120 μsec . Measured chronaxies and model data suggest, that pulse durations $<60 \mu\text{sec}$ lead to a focusing of the neurostimulation effect on smaller diameter axons close to the electrode while avoiding stimulation of distant pyramidal tract fibers.

Introduction

Deep brain stimulation of the subthalamic nucleus (DBS-STN) is an established surgical treatment for motor fluctuations or dyskinesia in Parkinson's disease (PD).^{1–3} The outcome critically depends on appropriate lead location⁴ and setting of stimulation parameters. Inadvertent leakage of current into adjacent fiber tracts, such as pyramidal fibers lateral to the STN,⁵ limits the therapeutic window (TW) by causing dysarthria or impaired fine motor skills.⁶ As a result, much research has been devoted to modeling and visualizing the electrical field of a given electrode position and parameter setting within the individual brain anatomy⁷ and to developing new stimulation hardware allowing more flexible shaping of the current distribution.⁸

Stimulation effects, however, also depend on the temporal characteristics of the stimulus waveform. The

threshold for activation of neural elements with different membrane excitability properties covaries with stimulus strength, and duration of the stimulus pulse. The nonlinear interdependence of stimulus amplitude and pulse duration is reflected by the so called “strength–duration–curve” or chronaxie relationship. The minimal amount of current necessary to excite a neural element at an infinitely long pulse width (PW) is termed rheobase current. Chronaxie is a measure of the excitability of neural elements and has been defined as the pulse duration equivalent to the double rheobase current on the strength–duration curve.

Experimental measurements have documented that axons have lower chronaxies than neuron cell bodies.⁹ Chronaxies for the beneficial effects of DBS have been estimated to be around 129 μsec for thalamic and around 151 μsec for pallidal stimulation^{10,11} which is well within

the range of myelinated axons. Here, we present chronaxie evaluations of STN-DBS using a novel neurostimulation system (Vercise[®]; Boston Scientific, Valencia, CA). In particular, we explored the clinical usefulness of stimulation at ultra-short pulse duration as physiological concepts suggest that stimulation at PW <60 μ sec could improve the selectivity of DBS for particular neural elements and lead to a better distinction between desirable and adverse stimulation effects.

Subjects and Methods

Four patients (two female, age 49–62 years), who had been implanted with the Vercise[®] neurostimulation system (Boston Scientific, Valencia, CA) for bilateral DBS-STN in PD, underwent an extended programming session of their DBS system in the practically defined medication off-state (>12 h medication withdrawal) 2–4 months after surgery. Patients were included into the extended monopolar review session for optimizing their stimulation parameters after having had a stable clinical response to STN-DBS of greater than 30% motor score reduction with conventional programming parameters for at least 1 month. Goal of the monopolar review session was to determine the clinically optimal pulse duration and amplitude setting at the monopolar contact previously selected for chronic stimulation at 60 μ sec PW. Efficacy of neurostimulation was assessed by comparing the severity of motor symptoms at the begin of the review session ON DBS to the preoperative Unified Parkinson's Disease Rating Scale, part III (UPDRS-III) in the medication off-state.

In all patients' correct lead positioning had been verified by fusing the preoperative stereotactic MRI and chronic (≥ 40 days) postoperative CT using the stereotactic planning software (Leksell SurgiPlan, Elekta, Sweden). The mean AC-PC based coordinates of active contacts of the right hemisphere were 12.1 ± 0.8 mm lateral to AC-PC, 2.14 ± 1.37 mm below AC-PC, 1.62 ± 0.7 mm posterior to MCP, and of left hemispheric active contacts 13.4 ± 0.59 mm lateral, 2.9 ± 1.3 mm below and 1.4 ± 0.8 mm posterior.

For the monopolar review session we defined the efficacy threshold of DBS as the minimal current necessary to achieve complete or almost complete suppression of contralateral rigidity (corresponding to a UPDRS item 22 score of 0 or 1) and the adverse effect threshold as the minimal current inducing clinically noticeable side effects (e.g., muscle contraction). In random order we assessed the TW for the pulse durations 20, 30, 40, 50, 60, 90, and 120 μ sec at a frequency of 130 Hz by quickly ramping up current until adverse effects were noted and carefully titrating the current to determine the exact threshold. Thereafter, current was lowered until contralateral arm

rigidity returned to baseline severity (efficacy threshold). If no adverse effect could be encountered after increasing amplitude to 10 mA, testing was suspended and no TW could be determined. TW (in mA) was calculated for each tested PW by subtracting the efficacy threshold from the side effect threshold. For comparison between subjects TWs were normalized to the TW at 60 μ sec.

We calculated the chronaxies from the threshold currents for suppression of rigidity and muscle contractions by linearizing the strength–duration curves and estimating slope and intercept.¹²

Computational model of axonal activation

An idealized DBS model was constructed to assist in the interpretation of the clinical results. The model system consisted of a finite element electric field model of the DBS electrode, coupled to populations of multicompartment cable models of myelinated axons. Our previous work described the specific parameters of the electric field model¹³ and axon models.¹⁴ The effects of the DBS electric field on the axons were simulated using methods originally described by McNeal,¹⁵ adapted to specifically address modulation of the DBS waveform.¹⁶ Our simulations evaluated DBS of two distinct pathways near the DBS electrode. One pathway consisted of smaller (2 μ m) diameter axons located closer (1–2 mm) the electrode, while the other pathway consisted of larger (5.7 μ m) diameter axons located farther from (4–5 mm) the electrode. The threshold current for action potential initiation was calculated for each axon model in each pathway, as a function of the PW.

Results

The patients had a mean UPDRS-III motor score improvement from 51 ± 11.97 before surgery to 24.75 ± 8.58 points (–52%) in the medication off-state with STN-DBS.

During the monopolar review session we observed a clear inverse relationship between PW and side effect thresholds in all patients. Mild contractions or fasciculations in hand or face muscles were elicited in all cases and served to determine the threshold for activation of pyramidal tract fibers. We did not notice other stimulation induced adverse effects below this threshold in any patient. Complete determination of TW was possible for seven implanted electrodes due to a lack of testable rigidity contralateral to one. The TW was 2.2 ± 1.6 mA (median 2.3; range 3.9) at 60 μ sec, which proportionally increased by $182 \pm 128\%$ (median 160%; range 341%) at 30 μ sec, while decreasing by $46 \pm 28\%$ (median 34%; range 84%) at 120 μ sec (Fig. 1). At 20 μ sec PW

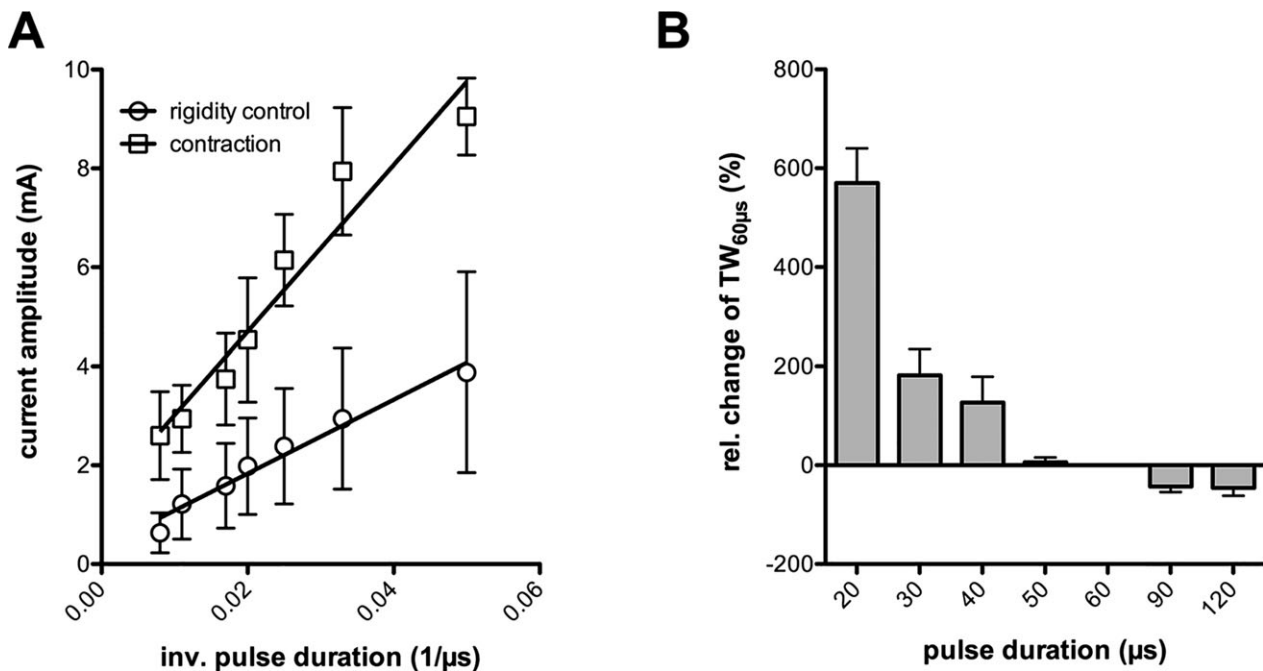


Figure 1. (A) linearized strength–duration curves for rigidity control and muscle contractions. (B) Bar graph depicting the relative change in therapeutic window compared to 60 μsec pulse duration ($\text{TW}_{60 \mu\text{sec}}$). Error bars indicate the standard error of mean in both graphs.

assessment of the TW was unreliable, because we could not elicit a capsular response for 6/8 electrodes below our testing limit of 10 mA.

The threshold current for complete rigidity control increased from 1.6 ± 0.9 (median 1.5; range 2.4) mA at 60 μsec to 2.9 ± 1.4 (median 2.8; range 3.6) mA at 30 μsec but the calculated total charge delivered per pulse was actually lower: 95 ± 51 (median 90; range 14) nC/pulse at 60 μsec versus 88 ± 43 (median 84; range 108) nC/pulse at 30 μsec ; -7%).

For both strength–duration curves we found a significant linear regression fit (rigidity control: $r = 0.97$; contractions: 0.94), when plotting mean threshold amplitudes against the inverse of pulse duration (Fig. 2). The slopes of the two regression lines were significantly divergent (74.8 ± 5.8 vs. 168.4 ± 19.0 ; $P < 0.0001$) indicating the stimulation of neural elements with different membrane excitability. From the mean and confidence range of the slopes we determined a chronaxie of 225 μsec (95% confidence range: 180–270 μsec) for the suppression of rigidity and 126 μsec (95% confidence range: 90–163 μsec) for muscular contractions.

Discussion

This is the first systematic analysis of the impact of pulse duration on therapeutic and adverse effects of subthalamic deep brain stimulation.

We found, that the TW of subthalamic neurostimulation increased up to twofold when using an ultra-short PW of 30 μsec compared to the standard PW setting of 60 μsec , currently suggested for STN-DBS programming.⁶ At 20 μsec pulse duration we could not elicit any capsular response below our upper testing limit of 10 mA in 6/8 electrodes suggesting an even better benefit/risk ratio. As expected, the efficacy threshold in mA increased at shorter pulse durations, but the total charge per pulse required for full rigidity control did actually decrease, suggesting that short PW stimulation may not only offer less risk of inducing stimulation induced adverse effects but also improve the energy efficiency of DBS. This would result in greater longevity of primary cell devices or expanded charging cycles of rechargeable pulse generators.

The estimated chronaxie of 168 μsec for muscle contraction is well below the limit of $<200 \mu\text{sec}$ for fast conducting pyramidal tract fibers, whereas a chronaxie of 222 μsec for rigidity suppression indicates stimulation of smaller axons with values between 200 and 700 μsec .⁹ In order to assist in the interpretation of these clinical results, we devised a computational model consisting of a finite element electric field model of the DBS electrode, coupled to populations of multicompartment cable models of myelinated axons.^{17,18} The effects of the DBS electric field on the axons were simulated using methods originally described by McNeal,¹⁵ adapted to specifically

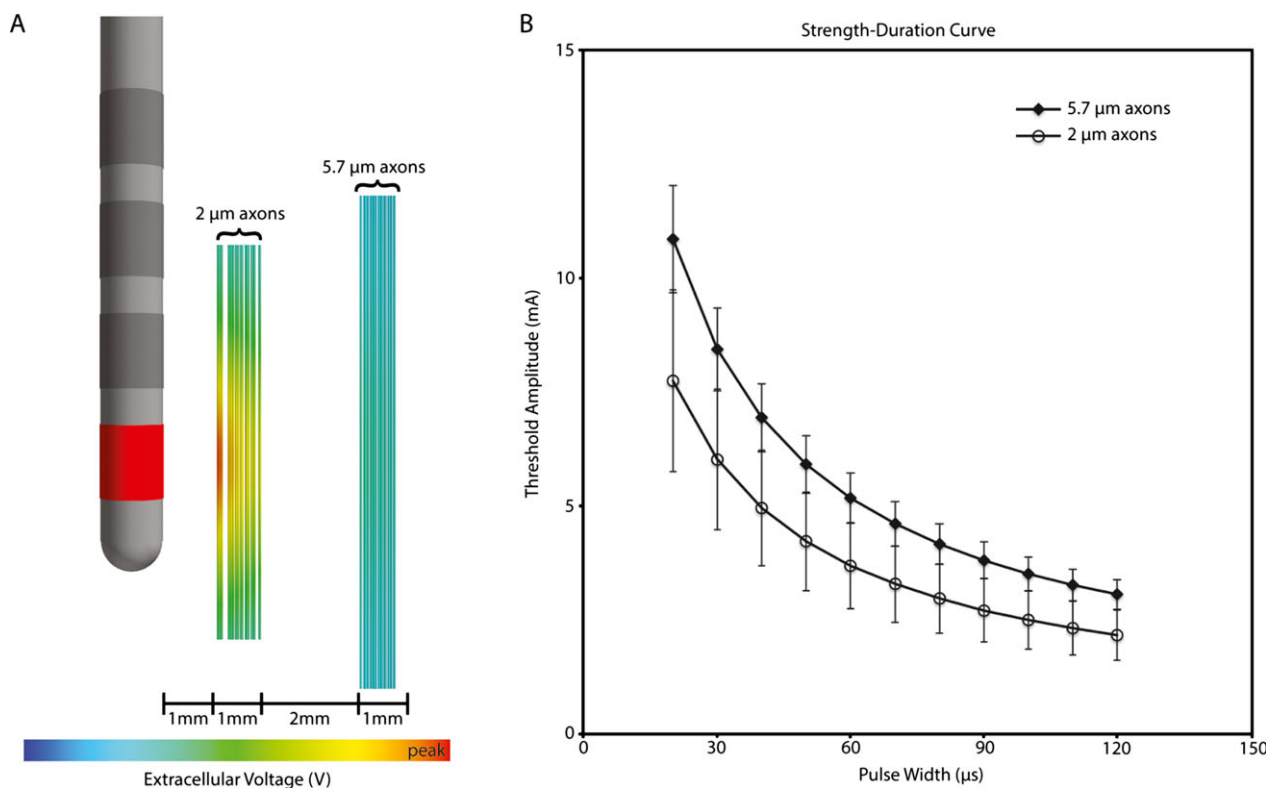


Figure 2. Model derived strength–duration curves for action potential initiation in smaller (2 μm) diameter axons located closer (1–2 mm) the electrode as compared to larger (5.7 μm) diameter axons located farther from (4–5 mm) the electrode. At shorter pulse duration the two curves diverge explaining an increased “therapeutic window” if benefit was associated with stimulation of the nearby fibers and adverse effects with the distant thick myelinated axons.

address modulation of the DBS waveform.¹⁶ In keeping with the chronaxie data, our simulations evaluated DBS of smaller (2 μm) diameter axons located closer (1–2 mm) and larger (5.7 μm) diameter axons located farther (4–5 mm) from the electrode corresponding to the approximate distance of the pyramidal tract. The current thresholds for generating a propagating axon potential predicted by the model reproduced the marked increase in TW at pulse durations below 60 μsec (Table 1). Hence, the mechanism of stimulation at short pulse duration may be best explained by focusing on excitation of smaller myelinated axons near the electrode and a steeper falloff for activation of thick myelinated axons with increasing radius of current spread.

Our chronaxie measurements do not allow us to explicitly determine the anatomical nature of the fibers responsible for rigidity control. The chronaxie could represent excitation of a single fiber pathway or a mixed effect of multiple fibers in the subthalamic area, such as corticosubthalamic fibers, pallidothalamic fibers dorsal to the STN or pallidosubthalamic fibers crossing the internal capsule. Rodent models, however, suggest antidromic

driving of corticosubthalamic fibers (“hyperdirect pathway”) and subsequent retuning of motor cortical spike firing as critical for the antiparkinsonian effect of subthalamic neurostimulation.^{19,20} In the rat the hyperdirect pathway consists of thin collaterals of fast conducting pyramidal tract axons originating from the frontal cortex deep layer V neurons.²¹ First imaging studies in humans did indeed visualize the “hyperdirect” pathway as a small bundle traveling along the internal capsule with the highest connectivity in the dorsolateral portion of the STN.²² Hence, programming in STN-DBS could face the dilemma of needing some current spread into the internal capsule for optimal coverage of those pyramidal tract collaterals, while at the same time avoiding inadvertent stimulation of adjacent corticospinal and corticobulbar fibers.

Our data suggest that this may be best achieved by stimulating at pulse durations below 60 μsec . A limitation may be the small number of patients investigated. However, the results were consistent and the strength–duration relation is a well-known physiological phenomenon, which was only reproduced in this study. Variability in our measures could result from the unblinded clinical

Table 1. Measured and model estimated threshold amplitudes for rigidity control and muscle contractions (capsular response) at different pulse durations.

Pulse width (μ sec)	Threshold amplitude (mA)			
	Patient data		Model data	
	Rigidity control	Capsular response	2 μ m axon	5.7 μ m axon
20	3.88 \pm 2.03	9.05 \pm 0.78	7.75 \pm 1.99	10.85 \pm 1.17
30	2.94 \pm 1.43	7.94 \pm 1.30	6.03 \pm 1.55	8.43 \pm 0.91
40	2.39 \pm 1.17	6.14 \pm 0.93	4.96 \pm 1.27	6.94 \pm 0.74
50	1.98 \pm 0.98	4.53 \pm 1.25	4.23 \pm 1.08	5.92 \pm 0.63
60	1.59 \pm 0.86	3.74 \pm 0.92	3.7 \pm 0.94	5.18 \pm 0.55
70	–	–	3.29 \pm 0.84	4.61 \pm 0.49
80	–	–	2.98 \pm 0.76	4.17 \pm 0.44
90	1.21 \pm 0.71	2.94 \pm 0.68	2.72 \pm 0.69	3.81 \pm 0.40
100	–	–	2.5 \pm 0.64	3.52 \pm 0.37
110	–	–	2.33 \pm 0.59	3.27 \pm 0.35
120	0.63 \pm 0.40	2.60 \pm 0.89	2.17 \pm 0.55	3.06 \pm 0.32

Values are given as mean \pm SD.

assessments, but neither rigidity nor fibrillations or contractions as a result of capsular stimulation can be reliably detected using objective methods.

A future clinical study including blinded assessments of stimulation effects on all Parkinsonian symptoms needs to ascertain this concept.

Author Contributions

Conception and design: J. Volkmann. Data collection: M. M. Reich, F. Steigerwald, A. Sawalhe, R. Reese, K. Gunalan, S. Johannes, C. Matthies. Data analysis: M. M. Reich, F. Steigerwald, K. Gunalan, C. C. McIntyre, J. Volkmann. Manuscript drafting: M. M. Reich, C. C. McIntyre, J. Volkmann. Critical revision of manuscript: all.

Conflict of Interest

Dr. Volkmann reports personal fees from Boston Scientific (Manufacturer of DBS systems), personal fees from Medtronic (Manufacturer of DBS systems), personal fees from St. Jude (Manufacturer of DBS systems), outside the submitted work.

References

1. Deuschl G, Schade-Brittinger C, Krack P, et al. A randomized trial of deep-brain stimulation for Parkinson's disease. *N Engl J Med* 2006;355:896–908.
2. Weaver FM, Follett K, Stern M, et al. Bilateral deep brain stimulation vs best medical therapy for patients with advanced Parkinson disease: a randomized controlled trial. *JAMA* 2009;301:63–73.
3. Williams A, Gill S, Varma T, et al. Deep brain stimulation plus best medical therapy versus best medical therapy alone for advanced Parkinson's disease (PD SURG trial): a randomised, open-label trial. *Lancet Neurol* 2010;9:581–591.
4. Wodarg F, Herzog J, Reese R, et al. Stimulation site within the MRI-defined STN predicts postoperative motor outcome. *Mov Disord* 2012;27:874–879.
5. Morel A, Magnin M, Jeanmonod D. Multiarchitectonic and stereotactic atlas of the human thalamus. *J Comp Neurol* 1997;387:588–630.
6. Volkmann J, Moro E, Pahwa R. Basic algorithms for the programming of deep brain stimulation in Parkinson's disease. *Mov Disord* 2006;21(suppl 14):S284–S289.
7. Butson CR, Cooper SE, Henderson JM, et al. Probabilistic analysis of activation volumes generated during deep brain stimulation. *NeuroImage* 2011;54:2096–2104.
8. Chaturvedi A, Foutz TJ, McIntyre CC. Current steering to activate targeted neural pathways during deep brain stimulation of the subthalamic region. *Brain Stimul* 2012;5:369–377.
9. Ranck JB. Which elements are excited in electrical stimulation of the mammalian central nervous system: a review. *Brain Res* 1975;98:417–440.
10. Holsheimer J, Demeulemeester H, Nuttin B, de Sutter P. Identification of the target neuronal elements in electrical deep brain stimulation. *Eur J Neurosci* 2000;12:4573–4577.
11. Holsheimer J, Dijkstra EA, Demeulemeester H, Nuttin B. Chronaxie calculated from current-duration and voltage-duration data. *J Neurosci Methods* 2000;97:45–50.
12. Groppa S, Herzog J, Falk D, et al. Physiological and anatomical decomposition of subthalamic

- neurostimulation effects in essential tremor. *Brain* 2014;137:109–121.
13. Butson CR, Moks CB, McIntyre CC. Sources and effects of electrode impedance during deep brain stimulation. *Clin Neurophysiol* 2006;117:447–454.
 14. McIntyre CC, Grill WM. Extracellular stimulation of central neurons: influence of stimulus waveform and frequency on neuronal output. *J Neurophysiol* 2002;88:1592–1604.
 15. McNeal DR. Analysis of a model for excitation of myelinated nerve. *IEEE Trans Biomed Eng* 1976;23:329–337.
 16. Foutz TJ, McIntyre CC. Evaluation of novel stimulus waveforms for deep brain stimulation. *J Neural Eng* 2010;7:066008.
 17. Butson CR, McIntyre CC. Differences among implanted pulse generator waveforms cause variations in the neural response to deep brain stimulation. *Clin Neurophysiol* 2007;118:1889–1894.
 18. McIntyre CC, Richardson AG, Grill WM. Modeling the excitability of mammalian nerve fibers: influence of afterpotentials on the recovery cycle. *J Neurophysiol* 2002;87:995–1006.
 19. Li Q, Ke Y, Chan DC, et al. Therapeutic deep brain stimulation in Parkinsonian rats directly influences motor cortex. *Neuron* 2012;76:1030–1041.
 20. Gradinaru V, Mogri M, Thompson KR, et al. Optical deconstruction of parkinsonian neural circuitry. *Science* 2009;324:354–359.
 21. Kita T, Kita H. The subthalamic nucleus is one of multiple innervation sites for long-range corticofugal axons: a single-axon tracing study in the rat. *J Neurosci* 2012;32:5990–5999.
 22. Brunenberg EJ, Moeskops P, Backes WH, et al. Structural and resting state functional connectivity of the subthalamic nucleus: identification of motor STN parts and the hyperdirect pathway. *PLoS One* 2012;7:e39061.